

Three-wave interactions and spatio-temporal chaos in the Faraday wave experiment

A.M. Rucklidge*

Department of Applied Mathematics, University of Leeds, Leeds LS2 9JT, UK

M. Silber†

*Department of Engineering Sciences and Applied Mathematics,
and NICO, Northwestern University, Evanston, IL 60208, USA*

A.C. Skeldon‡

Department of Mathematics, University of Surrey, Guildford GU2 7XH, UK

(Dated: May 12, 2022)

Three-wave interactions form the basis of our understanding of many nonlinear pattern forming systems because they encapsulate the most basic nonlinear interactions. In problems with two comparable length scales, such as the Faraday wave experiment with multi-frequency forcing, consideration of three-wave interactions can explain the presence of the spatio-temporal chaos found in some experiments, enabling some previously unexplained results to be interpreted in a new light. The predictions are illustrated with numerical simulations of a model partial differential equation.

PACS numbers: 47.54.-r, 47.52.+j, 05.45.-a, 47.35.Pq

In the Faraday wave experiment, patterns of standing waves are excited on the surface of a fluid by periodically shaking the fluids' container up and down. This deceptively simple experiment has been used extensively to provide insight into nonlinear pattern formation because it can be controlled easily and because it exhibits a rich variety of different phenomena: simple patterns such as stripes, squares and hexagons, as well as patterns with more complicated structure such as superlattice patterns, quasipatterns, oscillons and spatio-temporal chaos (STC) [1, 2]. Symmetry arguments and the consideration of three-wave interactions have played a key role in understanding some of the exotic patterns that arise [3–5]. Indeed, the variety of the observed behavior is due in part to the ability of the experimenter to tune in to different three-wave interactions by simply changing the forcing $f(t)$. Each frequency component in the forcing promotes the excitation of waves with different wavenumbers, thereby allowing different three-wave resonances.

Three-wave interactions have been invoked to explain the occurrence of superlattice patterns [6], where a pair of harmonic waves that are linearly excited by the forcing interact with a weakly damped harmonic wave related to a different component of the forcing. For example, in figure 1(a), two excited waves with wavevectors \mathbf{k}_1 and \mathbf{k}_2 on the outer circle (wavenumber 1) interact nonlinearly with a weakly damped wave whose wavevector \mathbf{q}_1 is on the inner circle (wavenumber q), as long as $\mathbf{k}_1 + \mathbf{k}_2 = \mathbf{q}_1$. The importance of this weakly damped wave is enhanced if it is driven harder (that is, if the amplitude of the appropriate component of the forcing is increased), and

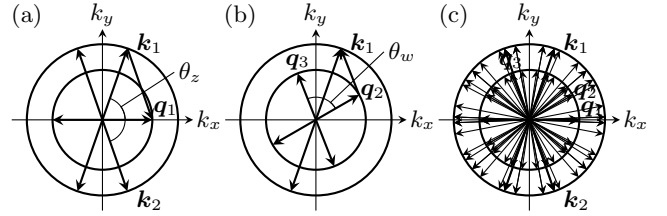


FIG. 1: Three-wave interactions between waves on two critical circles, with outer radius 1 and inner radius $q > \frac{1}{2}$. (a) A vector \mathbf{q}_1 on the inner circle can be written as the sum of two vectors \mathbf{k}_1 and \mathbf{k}_2 on the outer circle; this defines the angle $\theta_z = 2 \arccos(q/2)$. (b) The vector \mathbf{k}_1 is the sum of two inner vectors \mathbf{q}_2 and \mathbf{q}_3 ; this defines the angle $\theta_w = 2 \arccos(1/2q)$. (c) Similarly, \mathbf{k}_2 is the sum of two inner vectors, and each of these is in turn the sum of two outer vectors. In this example, $q = 0.66$, so $\theta_z = 141.4^\circ$ and $\theta_w = 81.5^\circ$.

patterns that contain the angle $\theta_z = 2 \arccos(q/2)$ can be stabilized [5]. This has been investigated experimentally [7–9], where the phases and amplitudes of the different components of the forcing are shown to determine whether the system produces simple patterns, superlattice patterns, quasipatterns or STC. The stabilization of some superlattice patterns can be understood entirely using this single three-wave interaction, but details of the origin of the STC are not well understood.

In this paper we extend the same notion of three-wave interactions to explain the origin of spatio-temporal chaos and other features of the experimental results of [8].

If $\frac{1}{2} < q < 1$, three-wave interactions also exist between two modes on the inner circle and one on the outer, as shown in figure 1(b). Two waves with wavevectors \mathbf{q}_2 and \mathbf{q}_3 on the inner circle interact with an outer vector \mathbf{k}_1 provided $\mathbf{q}_2 + \mathbf{q}_3 = \mathbf{k}_1$. This defines an angle $\theta_w = 2 \arccos(1/2q)$ between the two inner vectors. Similarly, \mathbf{k}_2 is the sum of two inner vectors, and each of these

*Electronic address: A.M.Rucklidge@leeds.ac.uk

†Electronic address: m-silber@northwestern.edu

‡Electronic address: A.Skeldon@surrey.ac.uk

inner vectors is in turn the sum of two outer vectors. For almost all choices of q , repeating this process generates an infinite number of vectors, resulting in the possible nonlinear interaction of infinitely many modes on both critical circles, as illustrated in figure 1(c).

There are two exceptions: when q is $\frac{1}{2}(\sqrt{5}-1) = 0.6180$ or $\frac{1}{2}(\sqrt{6}-\sqrt{2}) = 0.5176$, corresponding to $\theta_z = 2\theta_w = 144^\circ$ and $\theta_z = 5\theta_w = 150^\circ$, only a finite number of wavevectors on the critical circles are generated. These two special cases correspond to 10-fold and 12-fold quasipatterns respectively. The values of q that one might expect to lead to eight-fold patterns generate an infinite number of vectors. Hexagons and squares are also not exceptions: for example, if $q = 1/\sqrt{2}$, we have $\theta_w = 90^\circ$ (favoring squares perhaps) but $\theta_z = 138.6^\circ$, which does not fit in a square lattice.

There are several different ways that all these sets of three waves can interact, depending on whether the three-wave interactions favor mutual enhancement of the waves or competition between the waves. Starting with wavevectors \mathbf{k}_1 , \mathbf{k}_2 and $\mathbf{q}_1 = \mathbf{k}_1 + \mathbf{k}_2$, we write the pattern-forming field $U(x, y, t)$ as

$$U = z_1(t)e^{i\mathbf{k}_1 \cdot \mathbf{x}} + z_2(t)e^{i\mathbf{k}_2 \cdot \mathbf{x}} + w_1(t)e^{i\mathbf{q}_1 \cdot \mathbf{x}} + \text{c.c.} + \text{h.o.t.},$$

where the fast time dependence has been suppressed. This results (at lowest order) in the amplitude equations

$$\begin{aligned}\dot{z}_1 &= \mu z_1 + Q_{zw}\bar{z}_2 w_1 + \text{cubic terms}, \\ \dot{z}_2 &= \mu z_2 + Q_{zw}\bar{z}_1 w_1 + \text{cubic terms}, \\ \dot{w}_1 &= \nu w_1 + Q_{zz}z_1 z_2 + \text{cubic terms},\end{aligned}\quad (1)$$

where μ and ν are growth rates corresponding to wave-numbers 1 and q , and Q_{zw} and Q_{zz} are coefficients of the quadratic terms. We can write similar equations for the interaction between two waves on the inner circle, with wavevectors \mathbf{q}_2 and \mathbf{q}_3 , and one wave on the outer circle, with wavevector $\mathbf{k}_1 = \mathbf{q}_2 + \mathbf{q}_3$. If the mode amplitudes are w_2 , w_3 and z_1 , the amplitude equations are:

$$\begin{aligned}\dot{w}_2 &= \nu w_2 + Q_{wz}\bar{w}_3 z_1 + \text{cubic terms}, \\ \dot{w}_3 &= \nu w_3 + Q_{wz}\bar{w}_2 z_1 + \text{cubic terms}, \\ \dot{z}_1 &= \mu z_1 + Q_{ww}w_2 w_3 + \text{cubic terms},\end{aligned}\quad (2)$$

where Q_{wz} and Q_{ww} are more quadratic coefficients.

The dynamics of equations (1) (or equivalently (2)) with appropriate cubic terms has been explored by [10, 11] and others. The behavior of the system is influenced heavily by the signs of the quadratic coefficients. Based on arguments similar to those in [10], we find that if the quadratic coefficients have the same sign ($Q_{zz}Q_{zw} > 0$, or $Q_{ww}Q_{wz} > 0$ in (2)), there is enhanced stability of steady patterns with all three modes present and so the angle θ_z will be a feature of the pattern for a range of μ and ν . This is the typical scenario in many two-frequency Faraday experiments where the three-wave interaction is between two primary harmonic modes and a weakly damped harmonic difference frequency mode [6].

In contrast, if the quadratic coefficients have opposite sign, there is competition between the different modes, resulting typically in patterns with one wavevector being stable, or in time-dependent (possibly chaotic) oscillations of the amplitudes of the modes [10]. This also occurs in the Faraday experiment if the three-wave interaction involves 1 : 2 temporal resonance [6].

Putting these together, for $\frac{1}{2} < q < 1$, each mode on each circle will be influenced by two types of three-wave resonance: one type involving interaction with a pair of modes from the opposite circle, and the other involving interaction with one mode from each circle. (There is also the usual interaction between three waves at 120° .) Out of the resulting multitude of nonlinear interactions (see figure 1(c)), three different scenarios are to be expected depending on whether each type of three-wave resonance is enhancing or competitive, dictated by the signs of the products $Q_{zz}Q_{zw}$ and $Q_{ww}Q_{wz}$, as described above. If $Q_{zz}Q_{zw}$ and $Q_{ww}Q_{wz}$ are both positive, then either or both θ_z and θ_w will be reinforced, and steady patterns are to be expected. For the special values of q mentioned above we expect to see 10-fold or 12-fold quasipatterns. For other values of q , there could be complex spatial structure. If $Q_{zz}Q_{zw} > 0$ and $Q_{ww}Q_{wz} < 0$ (or the other way around), then θ_z is enhanced and θ_w is suppressed (or vice-versa), and we expect to see the corresponding superlattice patterns or quasipatterns. However, because of competitive three-wave interactions associated with the quadratic coefficients having opposite sign, we also expect to see time dependence and spatio-temporally chaotic competition between superlattice patterns of different orientations. If $Q_{zz}Q_{zw}$ and $Q_{ww}Q_{wz}$ are both negative, then we expect time-dependent competition leading to intermittent appearance of patterns with θ_z or θ_w , and possibly STC. In all cases the patterns that are seen will also depend on the growth rate parameters μ and ν , as well as on the cubic coefficients.

These scenarios provide an explanation of some of the observed Faraday wave phenomena in the experiments of [8]. These use three-frequency forcing:

$$f(t) = a_m \cos(m\omega t) + a_n \cos(n\omega t + \phi_n) + a_p \cos(p\omega t + \phi_p),$$

where one phase has been set to zero, and $(m, n, p) = (4, 5, 2)$ and $(6, 7, 2)$. The three-wave interactions are between harmonic modes, driven by the $(4, 2)$ and $(6, 2)$ components of the forcing, with the primary instability being to the larger frequency. The radius ratios are $q \approx 0.52$ and $q \approx 0.38$ in the two cases: these are the radius ratios that arise in 12-fold quasipatterns and 22° superlattice patterns. The presence of these two patterns as a function of the phases (ϕ_5, ϕ_2) and (ϕ_7, ϕ_2) is indicated by light areas in figure 2(a,b). The slopes of the bands and their periodicity are related to time translation symmetries of components of $f(t)$ [5].

The two cases, $(4, 5, 2)$ and $(6, 7, 2)$ excitation, differ in that in the first case, $q > \frac{1}{2}$, and ‘two-way’ resonance between the different critical modes is possible, whereas in the second case, $q < \frac{1}{2}$, and no such two-way resonance

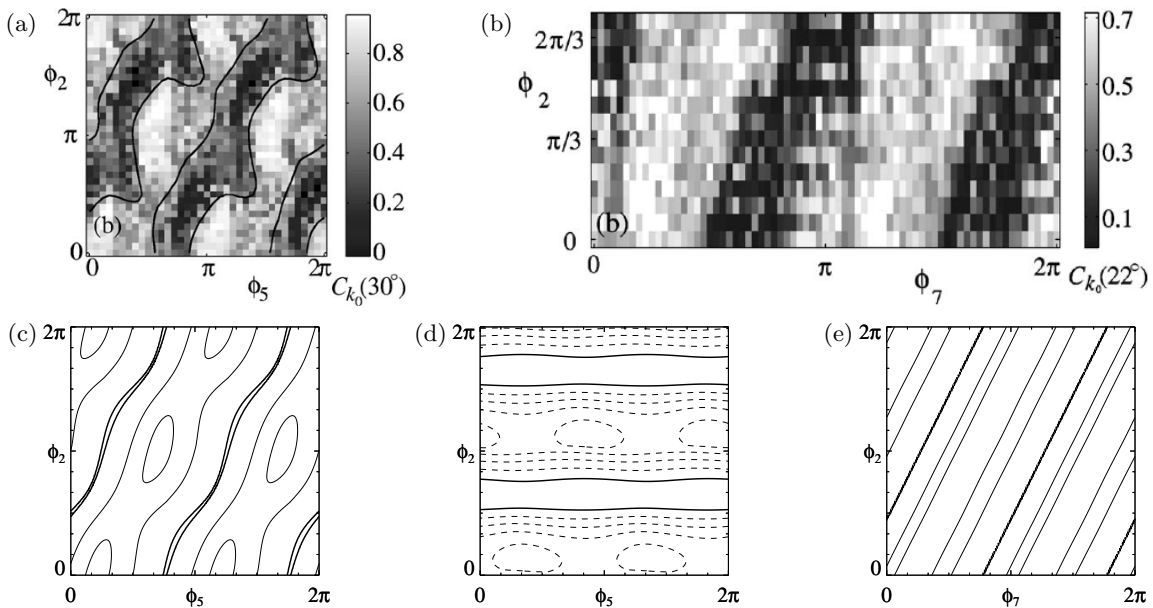


FIG. 2: (a,b) Experimental results of Ding and Umbanhowar [8], reproduced with permission. (a) The 30° angular autocorrelation function with $(4, 5, 2)$ forcing: white indicates 12-fold quasipatterns, as a function of (ϕ_5, ϕ_2) . Black indicates disordered patterns. (b) The 22° angular autocorrelation function with $(6, 7, 2)$ forcing: white indicates 22° superlattice patterns, as a function of (ϕ_7, ϕ_2) . (c,d,e) Products of quadratic coefficients, calculated from the Navier–Stokes equations using the methods of [12]. (c,d) Parameter values as in the experiment in (a), with (c) $Q_{zz}Q_{zw}$ (contours in steps of 0.2) and (d) $Q_{ww}Q_{wz}$ (contours in steps of 0.05) (e) Parameter values as in (b), showing $Q_{zz}Q_{zw}$ (contours in steps of 0.1). In all cases, the thick line is the zero contour, solid lines are positive contours, and dashed lines are negative contours.

can occur. We have calculated the values of the relevant quadratic coefficients using weakly nonlinear analysis of the Navier–Stokes equations for the experimental fluid parameters by extending the method in [12]. In figure 2(c,d), we show $Q_{zz}Q_{zw}$ and $Q_{ww}Q_{wz}$ for the $(4, 5, 2)$ case. Both products can take either positive or negative values, although $Q_{zz}Q_{zw}$ is negative only in narrow diagonal bands. In figure 2(e), we show $Q_{zz}Q_{zw}$ for the $(6, 7, 2)$ case. Comparing with the experimentally determined patterns in figure 2(a,b), we note that regions of 12-fold quasipatterns and 22° superlattice patterns correlate extremely well with regions of positive $Q_{zz}Q_{zw}$. Conversely, when $Q_{zz}Q_{zw}$ is small or negative, the correlation coefficient in the experiments is low and STC is seen [13]. The extra structure in figure 2(a) as compared to (b) is aligned with changes in $Q_{ww}Q_{wz}$ in figure 2(d), though shifted in phase from the expectations outlined above: we would have expected the strongest STC where both $Q_{zz}Q_{zw}$ and $Q_{ww}Q_{wz}$ are negative.

The broad agreement between the experiments and the calculated coefficients is remarkable, in spite of the fact that the calculations are carried out at the harmonic–harmonic codimension-two point, whereas the experiments are near but not at this point. In addition, the cubic coefficients, which we have not taken into account in this discussion, have an important effect [11].

We have further investigated the importance of the signs of the quadratic coefficients in the two-way resonance by devising a new model PDE based on the Swift–

Hohenberg equation [14] for a field $U(x, y, t)$:

$$\frac{\partial U}{\partial t} = \mathcal{L}(\mu, \nu)U + Q_1 U^2 + Q_2 U \nabla^2 U + Q_3 |\nabla U|^2 - U^3. \quad (3)$$

The model (3) is an extension of that of [15], modified to allow the growth rates of the two critical modes to be controlled independently. The linear part of the PDE \mathcal{L} acts on a mode e^{ikx} with eigenvalue $\sigma(k)$; we define \mathcal{L} by specifying how the eigenvalue should depend on k . Specifically, $\sigma(1) = \mu$ and $\sigma(q) = \nu$, controlling the growth rates of the modes of interest; $\sigma'(1) = \sigma'(q) = 0$; and $\sigma(0) = \sigma_0 < 0$ controls the depth of the minimum between $k = 1$ and $k = q$. With σ an even function of k , these requirements lead to a fourth-order polynomial in k^2 :

$$\sigma(k) = \frac{k^2 (A(k)\mu + B(k)\nu)}{q^4 (1 - q^2)^3} + \frac{\sigma_0}{q^4} (k^2 - 1)^2 (k^2 - q^2)^2,$$

where $A(k) = (k^2(q^2 - 3) - 2q^2 + 4)(k^2 - q^2)^2 q^4$ and $B(k) = (k^2(3q^2 - 1) + 2q^2 - 4q^4)(k^2 - 1)^2$. The linear operator \mathcal{L} is obtained by replacing k^2 by $-\nabla^2$. The nonlinear terms in the PDE model are simple quadratic and cubic combinations of U and its derivatives. Standard weakly nonlinear theory gives the values of Q_{zz} , Q_{zw} , Q_{ww} and Q_{wz} : having the three quadratic terms in (3) enables different sign combinations to be chosen in the amplitude equations (1) and (2).

Simulations of equation (3) were carried out on a 30×30 domain (identified by [16] as a suitable choice

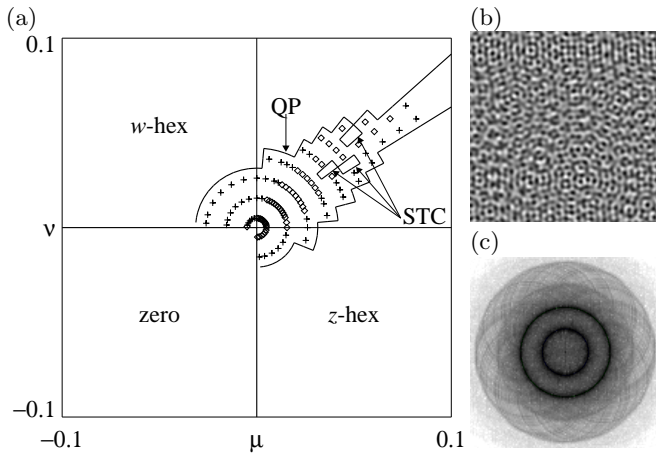


FIG. 3: (a) Bifurcation set showing the patterns that are seen for $q = 0.5176$, $\sigma_0 = -2$, $Q_1 = 0.3$, $Q_2 = 1.2$, $Q_3 = 1.4$ (so $Q_{zz}Q_{zw} < 0$ and $Q_{ww}Q_{wz} < 0$). Regions of stable z -hexagons ($k = 1$), w -hexagons ($k = q$), quasipatterns (QP), as well as spatio-temporal chaos (STC) are indicated. Steady quasipatterns are indicated with a +, time-dependent quasipatterns with a o. Hexagons are all steady and are not indicated for clarity. The (μ, ν) scale is not uniform. (b) Pattern for parameters in the innermost of the three STC regions, with $(\mu, \nu) = (0.0153, 0.0129)$. (c) The two critical circles are clearly seen in the power spectrum.

for approximate quasipatterns) for a range of different parameter values. Illustrative results are in figure 3(a) for $q = 0.5176$ and values of Q_1 , Q_2 and Q_3 that give $Q_{zz}Q_{zw} < 0$ and $Q_{ww}Q_{wz} < 0$, most relevant to the dark regions in figure 2(a). As well as stable hexagons, steady and time-dependent (chaotic) 12-fold quasipatterns are found when μ and ν are both positive and of comparable size. Windows of true STC are also found, with a typical solution shown in figure 3 (b,c). For other choices of q and the quadratic coefficients, the behavior of the PDE is broadly in line with the expectations specified above. When $q < \frac{1}{2}$, we find no examples of STC. For other values of $q > \frac{1}{2}$, we find steady and time-dependent examples of patterns with many modes

on both critical circles. In general, with both $Q_{zz}Q_{zw}$ and $Q_{ww}Q_{wz}$ positive, these patterns are all steady; time dependence (chaos or STC) is much more common when both $Q_{zz}Q_{zw}$ and $Q_{ww}Q_{wz}$ are negative. We find steady and time-dependent quasipatterns only with the special values $q = 0.5176$ and $q = 0.6180$, as discussed above. Further details will be presented elsewhere.

We conclude that whenever there are three-wave interactions between waves on two critical circles with radius ratio between $\frac{1}{2}$ and 2, interactions in both directions must be taken in to account. This is generic: we would expect these interactions to be important in other problems with two comparable length scales. Although we applied our results to explain patterns associated with a three-frequency Faraday wave experiment, we expect these interactions to be important even in two-frequency experiments. Most values of $q > \frac{1}{2}$ lead to the possibility of generating an infinite number of interacting waves. The exceptions are those values associated with 10- and 12-fold quasipatterns. The outcome of the mode interactions will be influenced by the signs of the quadratic coefficients in (1) and (2), with time-dependence and STC most likely in the case of both pairs of quadratic coefficients having opposite sign. By computing these coefficients from the Navier–Stokes equations, we have shown that this idea is in broad agreement with the experimental results of Ding and Umbanhowar [8]: as the phases in the forcing are varied, switches between 12-fold quasipatterns or 22° superlattice patterns and STC line up with changes of sign of the products of quadratic coefficients. This idea has been confirmed in our numerical investigation of a model partial differential equation (3).

Acknowledgments

We wish to acknowledge valuable conversations with Yu Ding, Jay Fineberg and Paul Umbanhowar. MS is grateful for support from the National Science Foundation (DMS-0709232).

-
- [1] H. Arbell and J. Fineberg, Phys. Rev. E **65**, 036224 (2002).
 - [2] A. Kudrolli, B. Pier, and J. P. Gollub, Physica D **123**, 99 (1998).
 - [3] W. S. Edwards and S. Fauve, J. Fluid Mech. **278**, 123 (1994).
 - [4] W. B. Zhang and J. Viñals, Phys. Rev. E **53**, R4283 (1996).
 - [5] J. Porter, C. M. Topaz, and M. Silber, Phys. Rev. Lett. **93**, 034502 (2004).
 - [6] C. M. Topaz, J. Porter, and M. Silber, Phys. Rev. E **70**, 066206 (2004).
 - [7] T. Epstein and J. Fineberg, Phys. Rev. E **73**, 055302(R) (2006).
 - [8] Y. Ding and P. Umbanhowar, Phys. Rev. E **73**, 046305 (2006).
 - [9] T. Epstein and J. Fineberg, Phys. Rev. Lett. **92**, 244502 (2004).
 - [10] J. Porter and M. Silber, Physica D **190**, 93 (2004).
 - [11] J. Guckenheimer and A. Mahalov, Physica D **54**, 267 (1992).
 - [12] A. C. Skeldon and G. Guidoboni, SIAM J. Appl. Math. **67**, 1064 (2007).
 - [13] Y. Ding, *Personal communication*.
 - [14] J. Swift and P. C. Hohenberg, Phys. Rev. A **15**, 319 (1977).
 - [15] R. Lifshitz and D. M. Petrich, Phys. Rev. Lett. **79**, 1261 (1997).
 - [16] A. M. Rucklidge and M. Silber, SIAM J. Appl. Dynam. Syst. **8**, 298 (2009).